Tooth segmentation using dynamic programming-gradient inverse coefficient of variation

Anuar Mikdad Muad[1], Nur Sakinah Mohamed Bahaman[2], Aini Hussain[3], Mohd Yusmiaidil Putera Mohd Yusof[4]

[1,2,3]Center for Integrated Systems Engineering and Advanced Technologies (INTEGRA), Faculty of Engineering and Built Environment, Universiti Kebangsaan Malaysia, 43600 UKM Bangi, Selangor, Malaysia
[4]Center of Study for Oral & Maxillofacial Diagnostics and Medicine Studies, Faculty of Dentistry, Universiti Teknologi Mara, 47000 Sungai Buloh, Selangor, Malaysia

Article Info

ABSTRACT

Teeth provide meaningful clues of an individual. The growth of the teeth is correlated with the individual age. This correlation is widely used to estimate age of an individual in applications like conducting forensic odontology, immigration, and differentiating juveniles and adolescents. Current forensic dentistry largely depends on laborious investigation process that is performed manually and can be influenced by human factors like fatigue and inconsistency. Digital panoramic radiograph dental images allow noninvasive and automatic investigation to be performed. This paper presents analyses on third molar tooth segmentation for the population in Malaysia, ranging from persons age of 5 years old to 23 years old. Two segmentation techniques: gradient inverse coefficient of variation with dynamic programming (DP-GICOV) and Chan-Vese (CV) were employed and compared. Results demonstrated that the accuracy of DP-GICOV and CV were 95.3%, and 81.6%, respectively.

Corresponding Author:

Anuar Mikdad Muad,
Center for Integrated Systems Engineering and Advanced Technologies (INTEGRA),
Faculty of Engineering and Built Environment, Universiti Kebangsaan Malaysia,
43600 UKM Bangi, Selangor, Malaysia.
Email: anuar_muad@ukm.edu.my

1. INTRODUCTION

The development of a human body can be measured with the biological age as its indicator. The biological age of an individual may not be the same with his or her chronological age, due to development variations of the body. Development of dental, bone, menarche, voice change, height, and weight can be used as variables to measure the biological age of the human body. The development of dental is more reliable than other variables to indicate the biological maturity in children and also more resistant than bones in the taphonomic process [1]. The measurement of the biological age based on dental can be associated with chronological age of an individual. The effort to associate the dental age with chronological age can be traced back to the year 1837 when an English dentist, Edwin Saunders presented a pamphlet entitled "The Teeth a Test of Age" in the British Parliament. His writing was related to child labor in factories in the United Kingdom [2]. Dental age estimation is an important information for forensic odontologist in order to assist government agencies and authorities to solve several cases, such as, determining the legal age for child in employment and criminal law or their eligibility to receive social benefits, processing undocumented immigrants, narrowing the search and identifying unknown victims.

The third molar is the most suitable teeth for dental age estimation in forensic investigation [3]. The third molar is related with the chronological age because it is the only tooth that still growing until late

adolescence, which can be regarded as legal age in the court of law. For an example, the legal age in the United States (US) is 18 years of age. Other countries may have different legal ages. Even so, the third molar growth display varying rates across races and sexes. In the US, the development of the third molar in American Hispanic is about one-half year earlier than American White, while for the American Black, their third molar develop one-half year earlier than American Hispanic [3]. Comparison between nine countries: Belgium, China, Japan, Korea, Poland, Thailand, Turkey, Saudi Arabia, and India also demonstrated significant differences in the development of the third molar. In addition, their finding also revealed that at all ages, the third molar growth of males is ahead of females [4]. Similar findings are also reported in China [5], Brazil [6], and Croatia [7]. All these studies suggest that the development of the third molar is influenced by ethnicity, hereditary, genders, nutrition, disease, medical treatments, habits, addictions, occupation, and other local effects. However, the most important factor is ethnicity and genders [3, 7].

There are methods to estimate the age from dental records [1], such as, morphological, biochemical, and radiological methods. Morphological method is the teeth assessment whereby the teeth need to be extracted from the human body. The morphological method examine the relationship between the chronological age and the changes in the dental tissue. These changes are attrition or tooth wear, periodontitis or gum diseases, secondary dentin, cementum apposition, root resorption, and transparency of the root [8,9]. Biochemical method involves amino acid racemization, an organic chemistry process that occur in dental biopsy to estimate the age of an individual [10, 11]. Biochemical is a multidisciplinary approach involving forensic odontology, biochemistry, histology and metric analysis [12]. Unlike the morphological method, biochemical method can be performed without extracting teeth. Radiology method uses panoramic x-ray dental images, which allow teeth investigation without removing the teeth form the body [5].

Radiology is an effective method because it is a noninvasive procedure and need not to remove the teeth from the body. The panoramic radiography images that are stored digitally can be analyzed using advanced image processing and other numerical techniques. Deep convolution neural network technique is used to perform teeth classification [13-16]. This automatic classification helps inexperience dentist to overcome the laborious task of manually recording the dental chart for corpses. Augmented reality and image registration techniques are used in dental surgery [17]. Image subtraction based segmentation is used to quantify leakage in dental restorations [18]. Multiple morphological gradient technique that consist of image dilation and erosion is employed to enhance the identification of proximal caries or tooth decay [19]. Volume rendering and texture analysis techniques are used to detect inferior alveolar nerve canal in dental implant surgery [20]. However, most of the image processing techniques are only focusing on teeth classification and did not relate the growth of the teeth with the chronological age of persons or victims.

In this paper, the segmentation of the third molar teeth is discussed. DP-GICOV [21] is employed in the segmentation and its results are compared with other segmentation technique, CV algorithm [22]. The segmentation is performed for a Malaysian dataset ranging on persons aged 5 years-old to 23 years-old. Results of segmentation are discussed with respect to the age ranges.

2.   RESEARCH METHOD
2.1. Panoramic radiography dental image

Digital images allow noninvasive analysis to be performed. In the forensic odontology, an example of a digital panoramic radiography dental image of a person is shown in Figure 1. Out of the many teeth, third molar or wisdom tooth is the most reliable indicator for age estimation. In a normal person, there are four third molar teeth as shown in four boxes in Figure 1. Two third molar teeth that are located at the upper dental jaw are not considered in this study because they tend to overlapped with their neighbors (i.e. second molar) as the person grow older. This situation may cause a complication in the image segmentation process. Only the third molar teeth at the lower dental jaw are considered because they are visibly apparent throughout the chronological development of a person and not affected by the overlapping problem by other teeth. Here, either one the teeth at the left or right can be used in the image processing of forensic odontology.
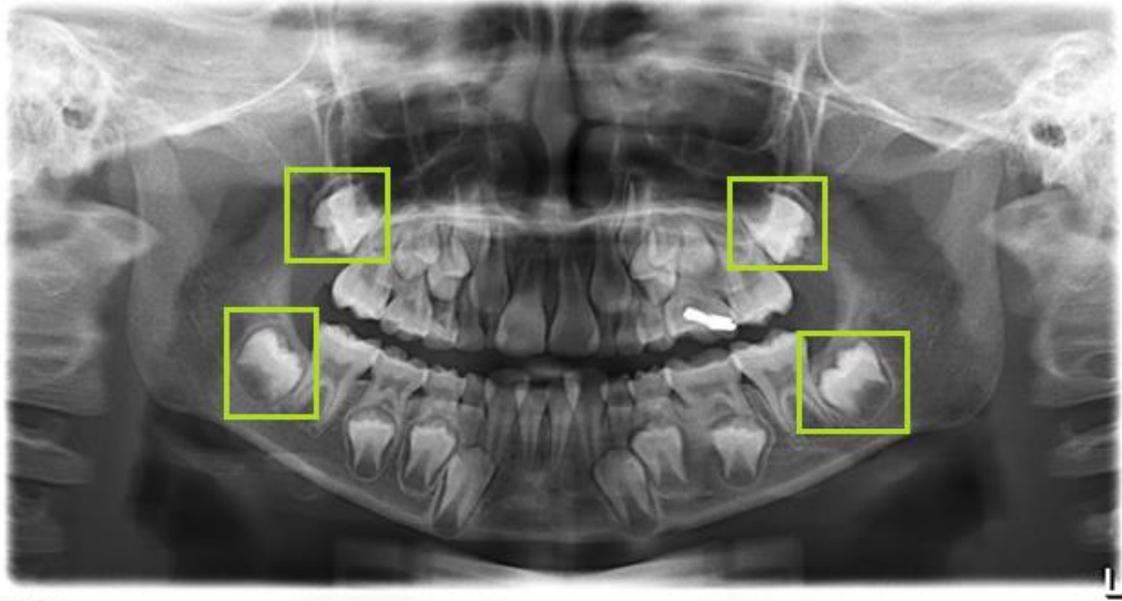
Figure 1. A panoramic radiography dental image

Four highlighted boxes show four wisdom teeth or third molar teeth. Only one of the teeth at the lower dental jaw is used in the image processing of forensic odontology.

2.2. Dynamic programming-gradient inverse coefficient of variation

Gradient inverse coefficient of variation (GICOV) measures the ratio of the mean and standard deviation of directional image derivatives over an entire closed contour fitted using active contour techniques to a tooth. GICOV operates by generating a number of radial lines originating from a centroid of the third molar tooth, which can be determined by users. Figure 2 shows a number of radial lines with different orientation from 0° to 360° angles. On each radial line, a number of sampling point is generated. Here, there are M radial lines, and N sampling points on each radial line.
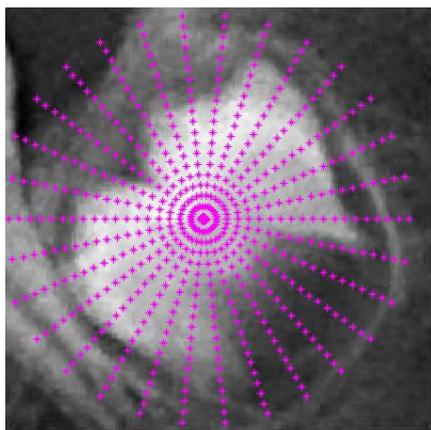
Figure 2. Generating M radial lines and N sampling point on each radial line. The centroid is manually defined by users
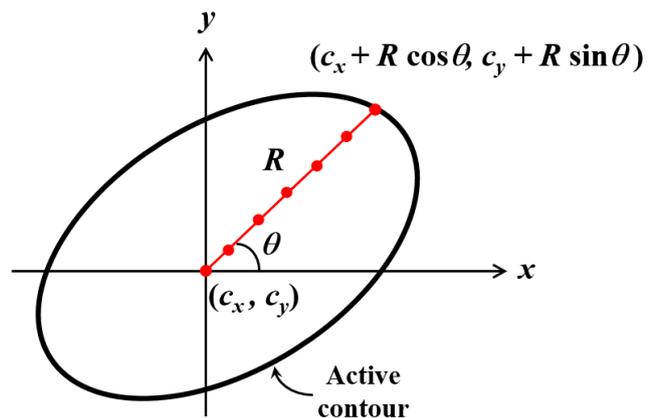
Figure 3. Converting Cartesian coordinate to polar coordinate

In order to focus the attention to the sampling points on every radial lines, the Cartesian coordinate of the contour points are converted to the polar coordinate as $(c_x + R \cos \theta, c_y + R \sin \theta)$ and shown in Figure 3. The gradient of the derivative images is computed as in (1).

$$\tilde{g} = \sqrt{I_x^2 + I_y^2} \qquad (1)$$

where $I_x = \partial I / \partial x$ and $I_y = \partial I / \partial y$. I is the image with polar coordinates. Further, directional information of the gradient is computed in (2)

$$g = \tilde{g} \cdot sign\left(I_x \cos\theta + I_y \sin\theta\right) \qquad (2)$$

where q is the angle of the radial line taken from a centroid of a two-dimensional closed contour. This centroid can be used as a point of initialization for the closed contouring method. The directional derivatives are the outward normal directions on contour points [21].

Figure 4(a) shows intensity profiles taken from point A to point B. This line denotes a radial line whereby point A is used as a centroid. Two plots from point A to B are drawn in Figure 4b, which shows the intensity plot of original image and the intensity plot of directional image gradient. Along the line from point A to B, dynamic programming (DP) [21, 23] is employed to determine a boundary point of the tooth, v_j. It is observed that the detection of the point v_j is easier by using the intensity of directional image gradient rather than the intensity of the original image.

(a)   (b)
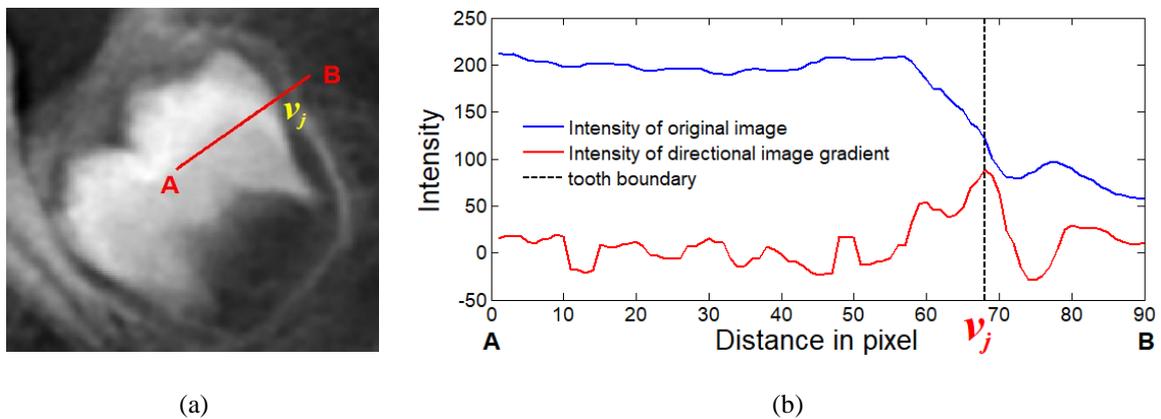
Figure 4. (a) A radial line generating from centroid, A to point B. vj is the boundary point of the tooth. (b) Intensity profiles for original image and directional image gradient taken from the centroid point, A to point B

GICOV score, G is the ratio of the mean and the variance of directional gradient, $g(u_1)$ at a point u_1 on the first radial line through, $g(u_N)$ at a point u_N on the N-th radial line as given in (3).

$$G(u_1,...,u_N) = \frac{\left(mean\left[g(u_1),...,g(u_N)\right]\right)^2}{\mathrm{var}\left[g(u_1),...,g(u_N)\right]} \qquad (3)$$

In order to maximize (3), this equation is rewritten as given in (4)

$$G = \frac{\left(\frac{1}{N}\sum_{i=1}^{N} g(u_i)\right)^2}{\frac{1}{N}\sum_{i=1}^{N} g(u_i)^2 - \left(\frac{1}{N}\sum_{i=1}^{N} g(u_i)\right)^2 + s} \qquad (4)$$

where s is the noise variance. The cost function of the active contour is given in (5).

$$E(v_1,\ldots,v_M) = E_1(v_1, v_2) + E_2(v_2, v_3) \\ + \ldots E_{M-1}(v_{M-1}, v_M) + E_M(v_M, v_1) \qquad (5)$$

(5) is computed using dynamic programming. Each cost function is defined in (6).

$$E = \begin{cases} g(v_i)^2 - 2cg(v_i) & \text{if } D(v_i, v_{i+1}) \leq \beta \\ \infty & \text{otherwise} \end{cases} \qquad (6)$$

where function $D(x)$ measures the distance between point v_i to point v_{i+1}, and b is the distance threshold.

Figure 5 shows the generation of the active contour from a linkage of points v_1, v_2, ... v_i, ... v_{M-1}, and v_M. Here, the combination of DP and GICOV is called DP-GICOV.
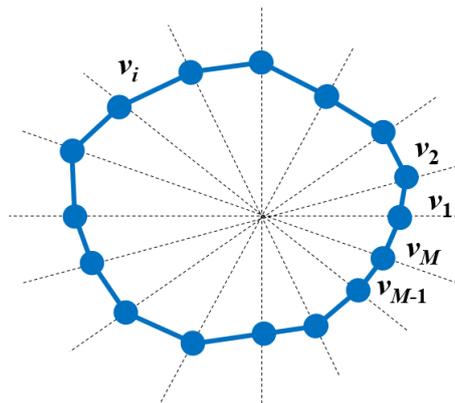
Figure 5. The dashed lines are the radial lines, and each radial line has a point, v_j indicating the boundary point of the tooth

All the points, v_1, v_2, ... v_i, ... v_{M-1}, and v_M are connecting with active contour using dynamic programming method.

2.3. Datasets

In order to conduct the current study, panoramic radiography dental images of living persons aged between 5 to 23 years old with no obvious developmental abnormalities are used. The sample are obtained from the Faculty of Dentistry, Universiti Teknologi Mara (UiTM). The third molar teeth either on the left or right of the lower dental jaw are analysed. Third molar of the upper dental jaw are not considered. Both erupted and non-erupted third molars are included in this study, as long as the third molar itself is distinguishable. The panoramic radiography dental images with the following anomalies are filtered out from this study: subjects with unknown dates of birth, subjects with missing third molar, subjects whom images could not be interpreted properly, and subjects with rotated third molar with large areas of enamel overlapped with neighbouring teeth. There are 650 images used in this study. Table 1 illustrate the distribution age of the samples.

Table 1. Distribution of the samples based on age group

Group	Age	No. of Samples
Group 1	5–7 years old	138
Group 2	8–10 years old	72
Group 3	11–13 years old	68
Group 4	14–16 years old	93
Group 5	17–19 years old	97
Group 6	20–23 years old	182
		Total: 650

Figure 6 shows samples of third molar teeth for the different age groups in order to demonstrate the morphological development of the third molar tooth. The stages of the tooth morphology starts with the appearance of the cusps tips, the merging of the cusps tips to form a well-defined coronal morphology, the formation of the crown, the appearance of the pulp chamber in a trapezoidal form, and the formation of the inter-radicular bifurcation. At this stage, the length of the root is less than the crown length. Then, the

development of the third molar continues with the expansion of the root length twice than the length of the crown. At this stage, the roots look like a funnel-shape ending. The root walls appear to be parallel, but tooth apices remain open. The development of the third molar concludes when apical ends of the roots are completely closed and periodontal ligament has a uniform width around the root. As shown in this figure, the progressive morphological growth of the third molar is correlated with the chronological age of an individual [3]. Images Figure 6 pose image processing challenges because contrast of a tooth is not uniform. At the crown part, the contrast is high between the tooth and the gum, but at the roots part, the contrast is relatively low. Figure 6f poses more difficult situation because the contrast of all the part of the tooth and the gum is very low. In addition to that, all the images appeared to be grainy, which might affect the accuracy of image segmentation.
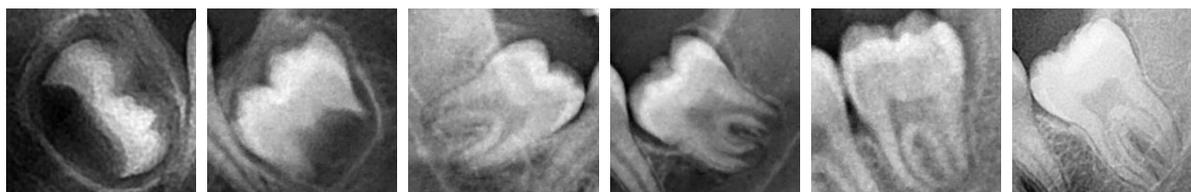
(a)   (b)   (c)   (d)   (e)   (f)

Figure 6. Samples of third molar teeth for persons aged (a) 5, (b) 10, (c) 13, (d) 15, (e) 18, and (f) 20 years old

3.   RESULTS AND ANALYSIS

Figure 7 shows results of DP-GICOV contour using different number of radial lines applied on a third molar tooth of a 10 year-old person. DP-GICOV requires suitable number of radial lines. If the number of radial lines are too small, the active contour of DP-GICOV is not able to track the boundary of the tooth. Using 300 lines allow the DP-GICOV to closely track the boundary. However some parts of the tooth, especially the roots of the tooth are not included in the contouring because the intensity contrast between the roots of the tooth and the gum is too low. The more radial lines are used, the slower the computational time for the DP-GICOV contour.
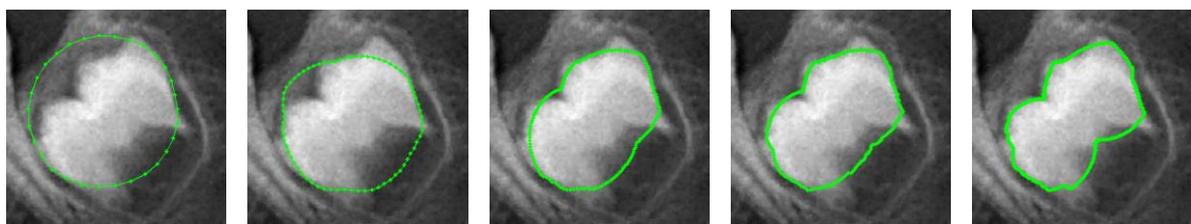
(a)   (b)   (c)   (d)   (e)

Figure 7. Results of DP-GICOV contour using different number of radial lines. (a) 30 radial lines, (b) 70 lines, (c) 150, (d) 200, and (e) 300 lines

Figure 8 shows results of segmentation using DP-GICOV and CV for samples of third molar teeth for different age groups. The segmentation accuracy of a sample from Group 1 (5 years old) using DP-GICOV is 94.2% and CV is 87.5%. Group 2 (10 years old)–DP-GICOV=96.1%, CV=89.5%. Group 3 (13 years old)–DP-GICOV=93.8%, CV=78.8%. Group 4 (15 years old)–DP-GICOV=93.5%, CV=80.0%. Group 5 (18 years old)–DP-GICOV=95.4%, CV=68.0%. Group 6 (20 years old)–DP-GICOV=93.5%, CV=72.8%. CV shows poor segmentation results whereby in all the images, this technique is heavily underestimated the boundary of the third molar. CV is severely influenced by the low contrast of the roots of the tooth and the gum, therefore, this part is not successfully segmented. Moreover, the effect of the grainy image also give rise to the inefficiency of the CV technique. Oppositely, DP-GICOV demonstrate close estimation of the boundary of the third molar. DP-GICOV is able to segment the roots of the tooth but rather inefficient to separate those roots. DP-GICOV demonstrates robustness when dealing with grainy images.

(a)   (b)   (c)   (d)   (e)   (f)
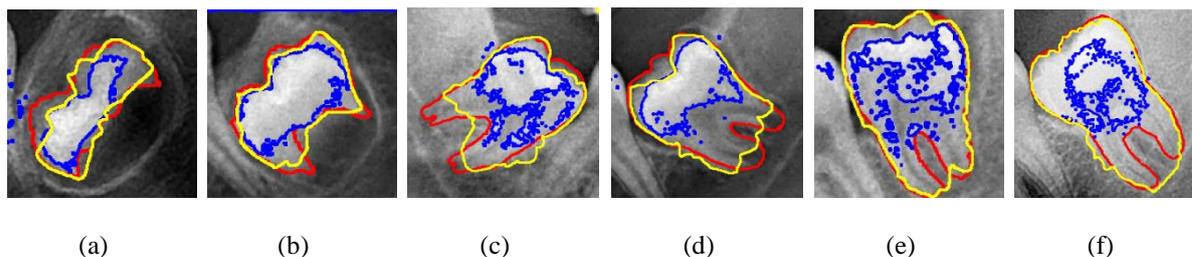
Figure 8. Segmentation results on the third molar tooth on persons aged (a) 5, (b) 10, (c) 13, (d) 15, (e) 18, and (f) 20 years old. Red, blue and yellow contours refer to the boundaries of ground truth, CV and DP-GICOV, respectively

Figure 9 shows the histograms of segmentation accuracy of DP-GICOV and CV for 650 third molar teeth samples that are divided into six age groups ranging from persons aged 5 years old to 23 years old. The morphology structure of the teeth changes as they undergo the teeth grow that is according to the chronological age of human being. From the histograms, there are two patterns between the accuracy of DP-GICOV and CV. DP-GICOV demonstrates a consistent pattern for all age groups. DP-GICOV is able to perform segmentation for approximately full shape of the third molar tooth across all the age groups and not influenced by the grainy effect of the image. On the other hand, CV shows decreasing trend of segmentation accuracy from Group 1 (5-7 years old) to Group 6 (20-23 years old). In the first two groups (Group 1 and Group 2), the roots are not fully emerged, therefore CV is able to produce high segmentation accuracy. However, in other age groups, when the roots of the tooth start to grow, CV experienced difficulty to perform segmentation between the roots and gum, because their intensity contrast is low, which deteriorates the segmentation accuracy. Overall, average accuracy of DP-GICOV is 95.3%, and CV is 81.6%.
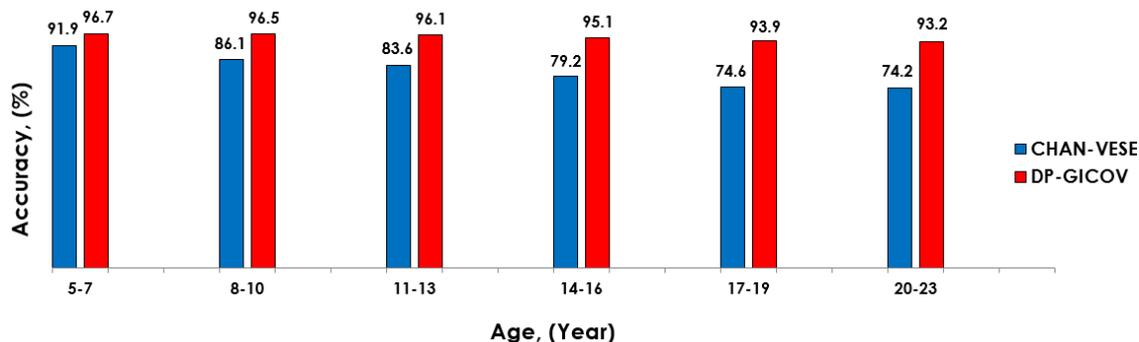
Figure 9. Results of classification accuracy of third molar teeth for persons aged from 5 to 23 years old

4.   CONCLUSION

Digital imaging allows noninvasive forensic odontologist analyses to be performed. Out of the many teeth, third molar or wisdom tooth is the most reliable indicator for age estimation. In this paper, the third molar tooth is segmented using DP-GICOV and CV techniques. Samples acquired from different age groups are used as they show variability in terms of morphological structure as persons grow older. DP-GICOV technique produces better segmentation results than that of the CV technique. For the future works, focus will be given on the estimation of age that relate with the shape of the tooth that has been segmented. The outcomes of this work can potentially be used to identify an individual or a victim in dental forensic investigation.

REFERENCES

[1]   Priyadarshini, C., Puranik, M.P. and Uma, S.R. Dental age estimation: A review, *International Journal of Advanced Health Sciences*. 2015; 1(12): 19-25.

[2]   Manjunatha, B.S. and Soni, N.K. Estimation of age from development and eruption of teeth. *Journal of Forensic Dental Sciences*. 2014; 6(2): 73-76.

[3]   Lewis, J.M. and Senn, D.R. Dental age estimation utilizing third molar development: A review of principles, methods, and population studies used in the United States. *Forensic Science International.* 2010; 201: 79-83.

[4]   Thevissen, P.W., Fieuws, S. and Willems, G. Human third molars development: Comparison of 9 country specific populations. *Forensic Science International.* 2010; 201: 102-105.

[5]   5 Guo, Y.C., Lia, M.J., Olze, A., Schmidt, S., Schulz, R., Zhou, H., Pfeiffer, H. and Chen, T. Studies on the radiographic visibility of the periodontal ligament in lower third molars: can the Olze method be used in the Chinese population? *International Journal of Legal Medicine*. 2018; 132(2): 617-622.

[6]   Lopes, L.J., Nascimento, H.A.R., Lima, G.P., dos Santos, L.A.N., Queluz, D.P. and Freitas, D.Q. Dental age assessment: Which is the most applicable method? Forensic Science International. 2018; 284: 97-100.

[7]   Galic, I., Lauc, T., Brkic, H., Vodanovic, M., Galic, E., Biazevic, M.G.H., Brakus, I., Badrov, J. and Cameriere, R. Cameriere's third molar maturity index in assessing age of maturity. *Forensic Science International.* 2015; 252: 191.e1-191.e5.

[8]   Schour, I. and Massler, M. The Development of Human Dentition. 2nd edition. Chicago: American Dental Association. 1994.

[9]   Kelmendi, J., Vodanovic, M., Kocani, F., Bimbashi, V., Mehmeti, B. and Galic, I. Dental age estimation using four Demirjian's, Chaillet's and Willems' methods in Kosovar children, Legal Medicine. 2018; 33: 23-31.

[10] Gustafson, G. Age determination of teeth, Journal of the American Dental Association. 1950; 41(1): 45-54.

[11] Adserias-Garriga, J., Thomas, C., Ubelaker, D.H. and Zapico, S.C. When forensic odontology met biochemistry: Multidisciplinary approach in forensic human identification, *Archive of Oral Biology*. 2018; 87: 7-14.

[12] Viciano, J., De Luca, S., Irurita, J. and Aleman, I. Age estimation of infants through metric analysis of developing anterior deciduous teeth, *Journal of Forensic Sciences*; 2017; 63(1): 20-30.

[13] Miki, Y., Muramatsu, C., Hayashi, T., Zhou, X., Hara, T., Katsumata, A. and Fujita, H. Classification of teeth in cone-beam CT using deep convolutional neural network. Computers in Biology and Medicine. Comput Biol Med. 2017; 80: 24-29.

[14] Kim, J.R., Shim, W.H., Yoon, H.M., Hong, S.H., Lee, J.S., Cho, Y.A. and Kim, S. Computerized bone age estimation using deep learning based program: Evaluation of the accuracy and efficiency, *Pediatric Imaging,* 2017; 209(6): 1374-1380.

[15] Larson, D.B., Chen, M.C., Lungren, M.P., Halabi, S.S., Stence, N.V. and Langlotz, C.P. Performance of a deep-learning neural network model in assessing skeletal maturity on pediatric hand radiographs, *Pediatric Imaging,* 2018; 289(1): 313-322.

[16] Spampinato, C., Palazzo, S., Giordano, D., Aldinucci, M. and Leonardi, R. Deep learning for automated skeletal bone age assessment in X-ray images, *Medical Image Analysis*, 2017; 36: 41-51.

[17] J. Wang *et al*., "Augmented Reality Navigation With Automatic Marker-Free Image Registration Using 3-D Image Overlay for Dental Surgery," in *IEEE Transactions on Biomedical Engineering*, vol. 61, no. 4, pp. 1295-1304, April 2014.

[18] Carrera, C.A., Lan, C., -Sanabria, D.E., Li, Y., Rudney, J., Aparicio, C. and Fok, A. The use of micro-CT with image segmentation to quantify leakage in dental restorations. *Dental Material*, 2015; 31(4): 382-390.

[19] Na'am, J., Harlan, J., Madenda, S. and Wibowo, E.P. Identification of the proximal caries of dental x-ray image with multiple morphology gradient method. *International Journal on Advanced Science Engineering Information Technology*, 2016; 6(3): 345-348.

[20] G. Kim *et al*., "Automatic Extraction of Inferior Alveolar Nerve Canal Using Feature-Enhancing Panoramic Volume Rendering," in *IEEE Transactions on Biomedical Engineering*, vol. 58, no. 2, pp. 253-264, Feb. 2011.

[21] Ray, N., Acton, S.T. and Hong, Z. *Seeing through clutter: Snake computation with dynamic programming for particle segmentation.* Proceedings of the 21st International Conference on Pattern Recognition. Tsukuba, Japan. 2012: 801-804.

[22] T. F. Chan and L. A. Vese, "Active contours without edges," in *IEEE Transactions on Image Processing*, vol. 10, no. 2, pp. 266-277, Feb. 2001.

[23] Ungru, K. and Jiang, X. Dynamic programming based segmentation in biomedical imaging, *Computational and Structural Biotechnology Journal,* 2017; 15: 255-264.